Preparation and Properties of Organic Radical Compounds with Mesogenic Cores

Shin'ichi Nakatsuji,*[a] Masako Mizumoto,[a] Hiroshi Ikemoto,[a] Hiroki Akutsu,[a] and Jun-ichi Yamada[a]

Keywords: Radicals / Biphenyl / Magnetic properties / Liquid crystals

Several organic spin systems based on 4-(*N*-alkyl)amino-TEMPO (TEMPO = 2,2,6,6-tetramethylpiperidinyl-1-oxy) radicals were prepared in which cholesterol or biphenyl mesogenic cores with long alkyl or alkoxy substituents were incorporated in order to investigate the possible occurrence of liquid crystalline properties. Of these radicals a lamellar structure was found in a biphenyl derivative with the 4-(*N*-methyl)amino-TEMPO-substituent **13**; this compound showed mesogenic properties. The local antiferromagnetic spin interactions based on a singlet-triplet model observed during the heating process in the radical were found to turn to a Curie–Weiss behavior after the thermal transition during the cooling process.

Introduction

The exploitation of novel molecule-based/organic magnetic materials with multi-functionality such as thermo- or photoresponsive magnetic properties is of current interest in the field of materials chemistry, and much attention has been paid in recent years to the preparation of such spin systems that show a synergy of the magnetic properties with outer stimuli such as heat or light.[1] During the course of our studies on the development of new organic magnetic materials,[2] we have been interested in preparing organic spin systems with conductivity, photofunctionality, liquid crystalline properties or pressure functionality.[3] The development of spin systems with liquid crystalline properties is particularly interesting because of the possibility of ordered spin interactions in the oriented molecular aggregates and/or the possibility of the alteration of the magnetic properties through the phase transition. We initiated our study by preparing spin systems with mesogenic cores as shown below.[4] It is known that sources of organic radicals are generally unsuitable for the synthesis of liquid crystals, due mainly to inappropriate substitution patterns or the geometry and bulkiness of radical stabilizing substituents, which are detrimental to mesophase stability;[5] only a few organic radicals with the less bulky DOXYL (4,4-dimethyl-3-oxazolidinyloxy) substituent have been reported to show liquid crystalline behavior.[6] We wish to report in this paper details of the preparation of several biradicaloid systems and a series of biphenyl carboxamide derivatives with 4-(*N*-alkyl)amino-TEMPO substituents and long alkyl or alkoxy substituents, their magnetic properties, the liquid crystalline property of the 4-(*N*-methyl)amino-TEMPO derivative **13** and its molecular/crystal structure.

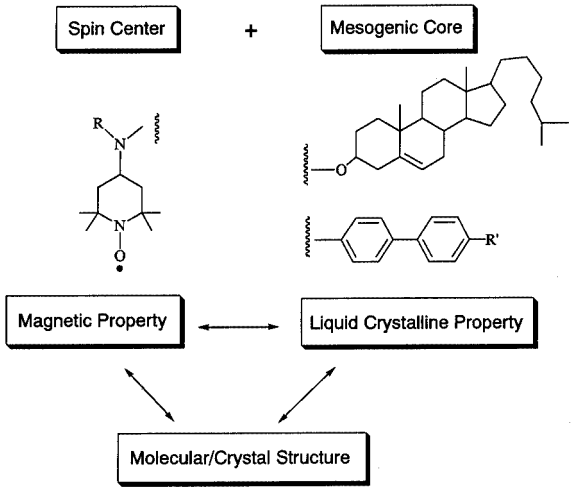

Results and Discussion

Preparation of Biradicals with a Cholesteryl or Biphenyl Moiety

Firstly, we tried to prepare some biradicaloid systems with two mesogenic cores since much interest is currently focused on liquid crystalline dimers (dimesogens) with two mesogenic units.[7] We then hoped to prepare the biradicals

[a] Department of Material Science, Faculty of Science, Himeji Institute of Technology,
3-2-1 Kouto, Kamigori, Hyogo 678−1297, Japan
Fax: (internat.) +81-791/58-0164
E-mail: nakatuji@sci.himeji-tech.ac.jp

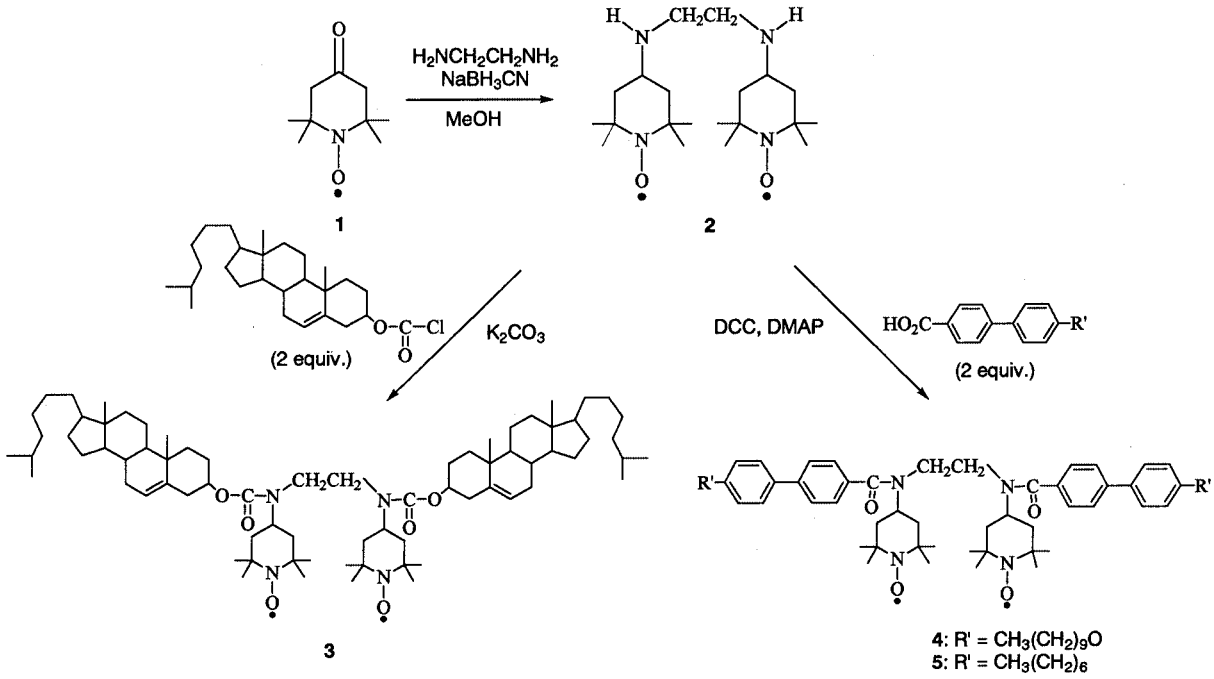

Scheme 1

with two cholesteryl (**3**) or biphenyl cores (**4** and **5**) by using bis-TEMPO-substituted ethylenediamine, which was obtained by the reductive amination of 4-oxo-TEMPO with ethylenediamine[8] as shown in Scheme 1.

Unfortunately, no liquid crystalline behavior was observed in the cholesteryl or in the biphenyl biradicaloid systems thus prepared when investigated by DSC or under a polarizing microscope.

Magnetic Properties of Biradicals 2−5 and the Molecular/Crystal Structure of 4

Magnetic susceptibility measurements were carried out for the biradicals **2**−**5** with a SQUID susceptometer in the temperature range from 2 K to 300 K. These data are summarized in Table 1. Only paramagnetic or weak antiferromagnetic interactions were observed in the biradicals, suggesting that the bulky substituents around the spin centers prevent strong magnetic interactions. Somewhat stronger interactions were observed in the spins of **4** with a Weiss temperature of −1.14 K (Figure 1).

A single crystal suitable for X-ray analysis was obtained for the biradical **4** by recrystallization from an ethanol/dichloromethane mixture. It was found from this analysis

Table 1. Magnetic data of biradicals

Compound	Magnetic interaction[a]	C [emu K mol^{-1}]	θ [K]
2	antiferromagnetic	0.54	−0.30
3	paramagnetic	0.72	0.00
4	antiferromagnetic	0.78	−1.14
5	antiferromagnetic	0.73	−0.28

[a] Fitting for Curie-Weiss law.

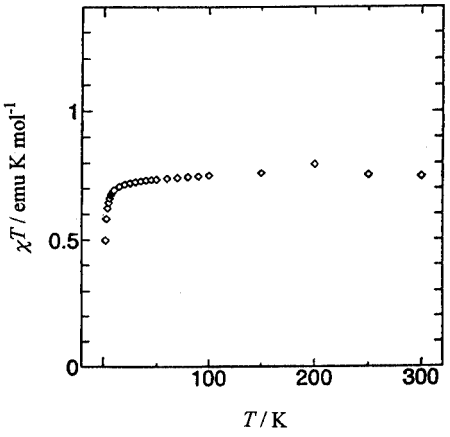

Figure 1. Temperature dependence of χT for biradical **4**

that two very similar but crystallographically independent molecules exist in the unit cell. Each six-membered ring of the TEMPO moiety in the biradical molecules protrudes from the long, rod-like molecular axis almost in a perpendicular manner and in an *anti* configuration. Such a TEMPO arrangement is supposed to be unsuitable for the formation of a mesogenic phase as it interferes with the aggregation of the molecules. Although the nearest intermolecular O−O distance between the radical centers is 6.09 Å, which is rather large for direct and strong spin-spin interactions, some short contacts are found between the aminoxyl groups and the carbon atoms of the aromatic or alkyl groups (as depicted in Figure 2), and these are thought to be the origin of the antiferromagnetic interactions observed in this biradical.[9]

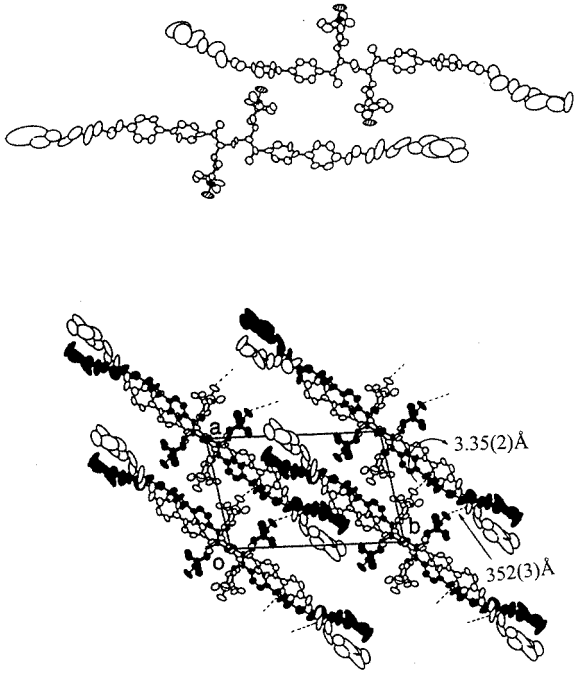

Figure 2. Top: molecular structure of **4** (two crystallographically independent molecules are depicted); bottom: crystal structure of **4** in which half parts of the two crystallographically independent molecules are depicted as closed circles and a couple of short contacts are indicated

Preparation of 4-(*N*-Alkyl)amino-TEMPO Radicals 6−9 and the Derived Monoradicals 10−19 with a Biphenyl Moiety

4-(*N*-Alkyl)amino-TEMPO derivatives with different chain lengths (**6−9**) were prepared in moderate yields by the reductive amination of 4-oxo-TEMPO (**1**) with several alkylamines using sodium cyanoborohydride as a reducing reagent (Scheme 2).

A series of monoradicaloid compounds with a biphenyl moiety (**10−19**) were synthesized from the 4-alkylamino-TEMPO derivatives **6−9** and 4-amino-TEMPO itself by reaction with the corresponding carboxylic acid derivatives and either DCC or DMAP, although the yields were not particularly high (Scheme 2).

An investigation of the thermal properties of the radicals **10−19** by DSC measurements revealed the possible existence of a mesogenic phase only in **13**. Thus, two endothermic profiles were observed in the DSC measurement of **13** during the heating process, indicating the existence of a mesophase at 374−377 K, although no reversibility was found during the cooling process. The appearance of a schlieren texture in the investigation with a polarizing microscope at around 375 K further supported the existence of a mesophase in the compound even though the range of this phase was found to be rather narrow.

Magnetic Properties of Monoradical Compounds 6−19, Molecular/Crystal Structure of 13, and Its Thermomagnetic Properties

As summarized in Table 2, only weak antiferromagnetic interactions were observed in all of the 4-(*N*-alkyl)amino-TEMPO radicals **6−9**, even in the radicals with long alkyl chains such as **8** or **9**. However, almost paramagnetic interactions were found in the 4-(*N*-methyl)amino-TEMPO derivative **6** and, although this compound seemed, at first glance, not to be a good spin center for spin-spin interactions when incorporated as a substituent, it later proved to be a significant system upon further investigation (vide infra).

The magnetic data of compounds **10−19** are also summarized in Table 2. Again, no significant magnetic interactions — only weak antiferromagnetic interactions — were observed in these compounds, except for radicals **12** and **13**. Rather similar magnetic behaviors based on a singlet-triplet (ST) model were found for **12** and **13** with almost the same *J* values of about 15 K. This behavior could not be anticipated because of the very weak magnetic interactions observed in the 4-*N*-methyl)amino-TEMPO radical itself (vide supra).

It was found from the X-ray analysis of **13** that there are two crystallographically independent molecules in the crystal (Figure 3). The TEMPO group on one molecule (the relative configuration for the carbonyl group and the *N*-

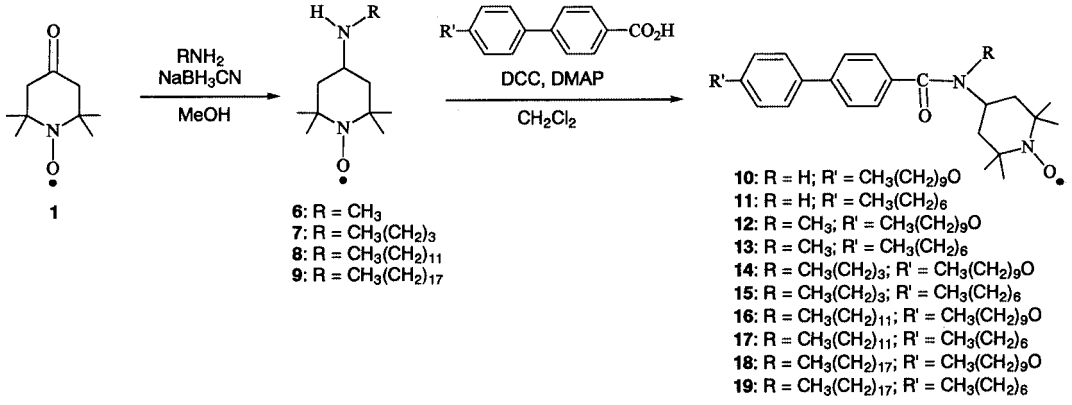

Scheme 2

Table 2. Magnetic data of monoradicals

Compound	Magnetic interaction	C [emu K mol^{-1}]	θ [K]	J [K]
6	paramagnetic[a]	0.33	−0.01	–
7	antiferromagnetic[a]	0.31	−0.79	–
8	antiferromagnetic[a]	0.31	−0.25	–
9	antiferromagnetic[a]	0.25	−0.97	–
10	antiferromagnetic[a]	0.38	−0.44	–
11	antiferromagnetic[a]	0.38	−0.67	–
12	antiferromagnetic[b]	–	–	−14.9
13	antiferromagnetic[b]	–	–	−14.8
14	antiferromagnetic[a]	0.38	−1.87	–
15	antiferromagnetic[a]	0.34	−0.50	–
16	antiferromagnetic[a]	0.38	−0.94	–
17	antiferromagnetic[a]	0.30	−0.42	–
18	antiferromagnetic[a]	0.38	−1.38	–
19	antiferromagnetic[a]	0.38	−2.80	–

[a] Fitting for Curie-Weiss law. [b] Fitting for singlet-triplet model.

methyl group is *syn*) is tilted to come close to the piperidine ring of another molecule (the relative configuration for the carbonyl group and the *N*-methyl group is *anti*) and there are short contacts between the oxygen atom in the aminoxyl moiety of the former molecule and the *N*-methyl group, as well as C(3) of the piperidine group of the latter molecule (3.36 Å and 3.49 Å, respectively). It is suggested from such structural features that the spin-spin interactions occur between the spin centers of the molecules through the hydrogen bond[10] between the oxygen atom of the aminoxyl group and the hydrogen on the *N*-methyl group and/or through the oxygen atom and a methylene carbon atom on the heterocyclic ring to afford local antiferromagnetic interactions, although the distances could not be rigorously estimated because the hydrogen atoms could not be refined in the X-ray analysis of compound **13**.[9]

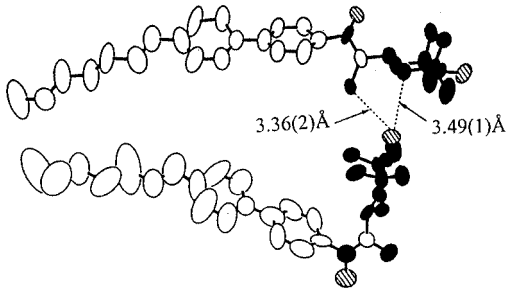

Figure 3. Two independent molecules of **13** in which short contacts are indicated between the oxygen atom of the aminoxyl moiety of one molecule and the carbon atoms of another molecule; the oxygen atoms are depicted as hatched circles and the carbon atoms of the TEMPO and carboxamide moieties are depicted as filled circles

The crystal structure of **13** viewed almost along the *a*-axis is shown in Figure 4 (left) and it is apparent that the molecules are stacking along the *c*-axis. Again, the short contacts described above between the two conformers follow an ST (dimer) model.

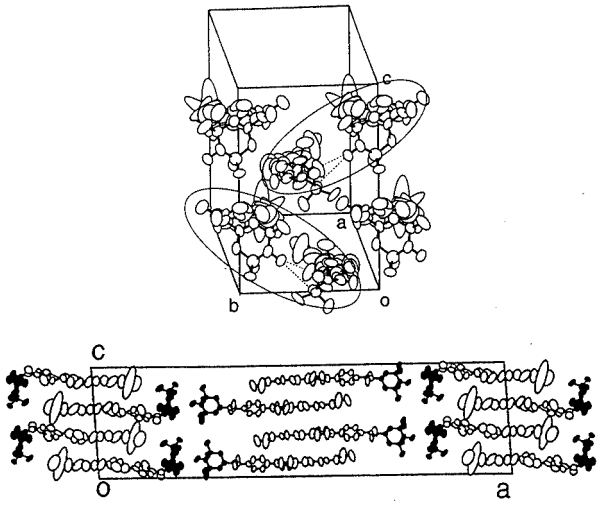

Figure 4. Top: Crystal structure of **13** viewed almost along the *a*-axis; paired molecules are shown in circles; bottom: crystal structure of **13** viewed along the *b*-axis in which TEMPO moieties are depicted as filled circles

The crystal structure of the same compound viewed along the *b*-axis is shown in Figure 4 (right) and it is apparent that there are two kinds of columns along the *c*-axis (actually in a zig-zag manner along the *b*-axis) consisting of two conformers in each of which the alkylbiphenyl and TEMPO groups stack separately and assemble asmongst themselves. This remarkable structural feature is similar to the lamellar structure of lyotropic liquid crystals or amphiphilic phospholipid bilayers in which the hydrophobic alkyl groups and hydrophilic phosphate groups stack separately.[11] Such a supramolecular structure in the crystal of **13** is essential for the significant antiferromagnetic interactions and the formation of a mesogenic phase in the compound.

We also measured the magnetic susceptibility of **13** in the range from 300 K to 393 K; these data are shown in Figure 5 (upper). The gradual decrease of the magnetic susceptibilities of **13** observed during the heating process was found to reverse at around 374 K; this temperature corresponds to the phase transition from the crystal phase to the mesophase.[12] This behavior suggests a change of the contribution of intermolecular interactions within the phase due mainly to a change in the molecular alignments, and it is presumed that the increasing strength of the intermolecular antiferromagnetic interactions during the heating process is abruptly released by the phase transition based on the structural change around the TEMPO moieties, which are relatively constrained in the crystal phase as shown in Figure 4. Thus, the magnetic behavior observed in the magnetic susceptibility measurements seems to reflect the occurrence of a heat-driven structural change in the crystal, which exhibits the mesophase at around 374 K. However, no appreciable decrease was observed during the cooling process (a gradual increase was observed instead) and this result is consistent with the DSC measurement with no endothermic peak during the cooling process.

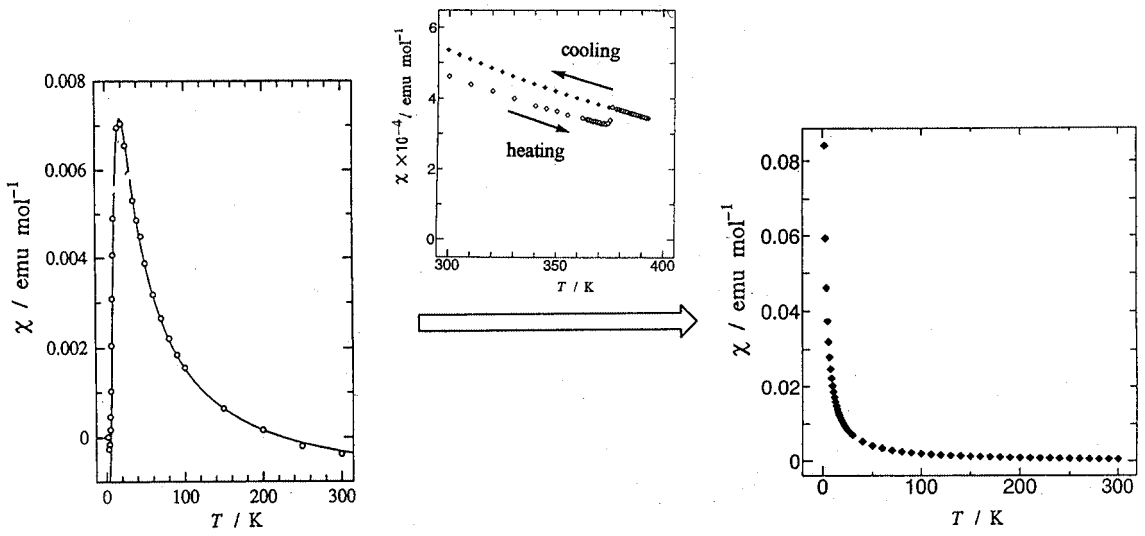

Figure 5. Temperature dependence of magnetic susceptibilities χ of **13** before (left) and after (right) the phase transition; the data between 300−393 K are shown in the middle figure; the plots of the heating and cooling process are depicted as open circles/diamonds and closed diamonds, respectively

Moreover, although the magnetic behavior can be well expressed by a singlet-triplet model with antiferromagnetic spin-spin interactions observed during the heating process, it was found to change to a Curie−Weiss behavior after the thermal transition during the cooling process as shown in Figure 5 (lower). Thus, the original magnetic behavior (ST) could be changed to another magnetic behavior (Curie−Weiss) by merely heating the radical over the thermal transition temperature, although a reverse change to the original behavior from the latter one was not observed in the further heating/cooling process.[13]

Conclusions

We have prepared a series of organic spin systems based on 4-(*N*-alkyl)amino-TEMPO radicals in which cholesteryl or biphenyl mesogenic cores with long alkyl or alkoxy substituents are incorporated, and we have investigated their magnetic and mesogenic properties. Among them, it was found from an X-ray analysis of the biradical compound **4** that the TEMPO moieties protrude from the long, rod-like molecular axis almost in a perpendicular manner, and with an *anti*-configuration, resulting in the absence of a mesogenic phase. On the contrary, a lamellar structure of the molecular packing feature was found in a biphenyl derivative with the 4-(*N*-methyl)carboxamido-TEMPO substituent **13**, giving a mesogenic behavior. The local antiferromagnetic spin interactions based on a singlet-triplet model were observed in this radical and the related radical **12**, while weak antiferromagnetic interactions were observed in other radicals; a paramagnetic behavior was found in the 4-(*N*-methylamino)-TEMPO radical itself. The magnetic behavior (ST model) observed during the heating process in the radical **13** was found to turn to a Curie−Weiss behavior after the thermal transition during the cooling process and thus exhibits an intriguing thermomagnetic property that is most likely derived from a change in its packing after the phase transition.

Experimental Section

Materials: 4-Oxo-TEMPO (**1**) 4-amino-TEMPO (**2**) alkylamines (ethylenediamine, methylamine, butylamine, dodecylamine, and octadecylamine), 4′-*n*-decyloxybiphenyl-4-carboxylic acid, and 4′-*n*-heptylbiphenyl-4-carboxylic acid are commercially available (Tokyo Kasei Kogyo Co.) and were used without further purification.

Instrumentation: Melting points were measured on a YAMATO MP-21 apparatus and are uncorrected. UV/Visible spectra were obtained on JASCO Ubest-35 spectrometer. MS spectra were taken using a JEOL JMS-AX 505 mass spectrometer. DSC data were obtained with Rigaku Thermal Analysis Station TAS100. Appearance of texture was investigated by a polarizing microscope, LABOPHOT2-POL with TH-1500MH heating apparatus. EPR spectra were obtained on a JEOL JES-FE3XG spectrometer and each g-value was determined using Mn^{2+}/MgO maker as internal standard. Susceptibility measurements were carried out on a Quantum Design MPMS-5 SQUID susceptometer using ca. 10 mg for each powdered sample in the usual way.[14]

X-ray Structure Determination: X-ray diffraction data were collected on a Rigaku RAXIS4 diffractometer with Mo-K_α radiation at room temperature. The structures were solved by direct methods and expanded using Fourier techniques. The non-hydrogen atoms were refined anisotropically. Hydrogen atoms were included but not refined. All calculations were performed using the teXsan.[15]

CCDC-174985 (**4**) and CCDC-174986 (**13**) contain the supplementary crystallographic data for this paper. These data can be obtained free of charge at www.ccdc.cam.ac.uk/conts/retrieving.html [or from the Cambridge Crystallographic Data Centre, 12, Union Road, Cambridge CB2 1EZ, UK; Fax: (internat.) +44-1223/336-033; Email: deposit@ccdc.cam.ac.uk].

Bis(4-amino-TEMPO)-Substituted Ethylenediamine Derivative 2: $NaBH_3CN$ (0.22 g, 3.6 mmol) was added to a stirred solution of oxo-TEMPO (0.87 g, 5.1 mmol) and ethylene-diamine·2HCl (1.7 g, 13 mmol) in absolute methanol (30 mL). After stirring for 3 days at ambient temperature, the solvent was concentrated in vacuo and then aqueous potassium hydroxide solution (5 N) was added (5 ml). The mixture was then extracted with dichloromethane, washed well with brine and the organic layer was dried over anhydrous magnesium sulfate. After evaporation of the solvent, the orange solid obtained was purified by column chromatography on silica gel (*n*-hexane/ethyl acetate/methanol) and then recrystallized from benzene to give radical **3** as orange needles (0.54 g, 29%), m.p. 117−120 °C. EPR (benzene): 3 lines, $g = 2.007$, $a_N = 1.55$ mT. $C_{20}H_{40}N_4O_2$ (368.58): calcd. C 65.00, H 10.58, N 15.00; found C 65.16, H 10.96, N 15.20.

Biradical 3 with a Bis(cholesteryl) Moiety: Cholesteryl chloroformate (0.30 g, 0.68 mmol) was added to a stirred solution of biradical **2** (0.11 g, 0.31 mmol) in chloroform (6 mL) followed by 40% potassium carbonate aq. solution and the reaction mixture was stirred at ambient temperature for 6 h. After extraction of the reaction mixture with chloroform, the organic layer was dried over anhydrous magnesium sulfate and then the solvent was evaporated in vacuo. The white solid thus obtained was purified by column chromatography on silica gel (*n*-hexane/benzene/ethyl acetate) and then recrystallized from benzene to give the biradical **3** as a white powdery solid (0.28 g, 76%), m.p. 213−215 °C. EPR (benzene): 3 lines, $g = 2.007$, $a_N = 1.56$ mT. $C_{76}H_{128}N_4O_6$ (1193.9): calcd. C 76.46, H 10.81, N 4.69; found C 76.55, H 10.70, N 4.31.

Biradicals 4 and 5 with a Bis(biphenyl) Moiety: DCC (0.42 g, 2.0 mmol) was added at ambient temperature to a stirred dichloromethane solution (30 mL) of **2** (0.34 g, 0.93 mmol), 4′-*n*-decyloxybiphenyl-4-carboxylic acid (0.66 g, 1.9 mmol), and DMAP (0.11 g, 0.93 mmol). The reaction mixture was stirred for 2 days at the same temperature and the resulting solid of urea was filtered off. The filtrate was then evaporated in vacuo to give a crude product, which was purified by column chromatography on silica gel (*n*-hexane/ethyl acetate) and recrystallized from ethanol/dichloromethane (1:1) to give **4** as orange needles (0.39 g, 20%), m.p. 166−168 °C. EPR (benzene): 3 lines, $g = 2.007$, $a_N = 1.56$ mT. $C_{66}H_{96}N_4O_6$ (1041.5): calcd. C 76.10, H 9.31, N 5.38; found C 76.28, H 9.24, N 5.18. The biradical **5** was prepared in a similar manner and isolated as orange crystals, m.p. 181−183 °C. EPR (benzene): 3 lines, $g = 2.007$, $a_N = 1.56$ mT. $C_{60}H_{84}N_4O_4$ (957.37): calcd. C 77.86, H 9.17, N 6.06; found C 78.25, H 9.15, N 5.79.

4-(*N*-Alkylamino)-TEMPO Radicals 6−9: The 4-(*N*-Alkylamino)-TEMPO radicals were prepared in a similar manner as described in the preparation of **2** by reductive amination of 4-oxo-TEMPO with alkylamines.

6: See ref.[16]

7: Yield 39%, orange crystals, m.p. < 20 °C. EPR (benzene): 3 lines, $g = 2.007$, $a_N = 1.56$ mT. FAB-MS: $m/z = 228$ [M + 2].[17]

8: Yield 76%, orange crystals, m.p. < 20 °C (decomp.). EPR (benzene): triplet, $g = 2.007$, $a_N = 1.56$ mT. FAB-HRMS: m/z (calcd. for $C_{21}H_{45}N_2O$): 341.3532; found 341.3541 [M + 2].[18]

9: Yield 68%, orange crystals, m.p. 39−42 °C (decomp.). EPR (benzene): 3 lines, $g = 2.007$, $a_N = 1.57$ mT. FAB-HRMS: m/z (calcd. for $C_{27}H_{57}N_2O$): 425.4471; found 425.4531 [M + 2].

Monoradicals 10−19 with a Biphenyl Core: The monoradicals **10−19** were prepared in a similar manner as described in the preparation of **4** and **5** by the condensation reaction of biphenyl-4-carboxylic acid with 4-(*N*-alkyl)amino-TEMPO radicals using DCC/DMAP

10: Yield 77%, orange powdery solid, m.p. 114−116 °C. EPR (benzene): 3 lines, $g = 2.007$, $a_N = 1.62$ mT. FAB-HRMS: m/z (calcd. for $C_{32}H_{47}N_2O_3$):451.3743; found 509.3690 [M + 2].

11: Yield 89%, orange powdery solid, m.p. 145−148 °C. EPR (benzene): 3 lines, $g = 2.006$, $a_N = 1.50$ mT. FAB-HRMS: m/z (calcd. for $C_{29}H_{41}N_2O_2$):451.3324; found 451.3252 [M + 2].

12: Yield 61%, orange powdery solid, m.p. 92−95 °C. EPR (benzene): 3 lines, $g = 2.007$, $a_N = 1.61$ mT. $C_{33}H_{49}N_2O_3$ (521.78): calcd. C 75.95, H 9.48, N 5.37; found C 76.01, H 9.36, N 5.34.

13: Yield 69%, orange plates, m.p. 97−99 °C. EPR (benzene): 3 lines, $g = 2.006$, $a_N = 1.49$ mT. $C_{30}H_{43}N_2O_2$ (463.69): calcd. C 77.69, H 9.36, N 6.04; found C 77.35, H 9.36, N 5.83.

14: Yield 57%, orange powdery solid, m.p. 90−95 °C. EPR (benzene): 3 lines, $g = 2.007$, $a_N = 1.56$ mT. FAB-MS: $m/z = 565$ [M + 2].

15: Yield 58%, orange oil, m.p. < 20 °C. EPR (benzene): 3 lines, $g = 2.007$, $a_N = 1.62$ mT. FAB-HRMS: m/z (calcd. for $C_{33}H_{49}N_2O_2$):507.3950; found 507.4006 [M + 2].

16: Yield 57%, orange powdery solid, m.p. 88−90 °C. EPR (benzene): 3 lines, $g = 2.006$, $a_N = 1.55$ mT. FAB-HRMS: m/z (calcd. for $C_{44}H_{73}N_2O_3$):677.5621; found 677.5583 [M + 2].

17: Yield 50%, orange oil, m.p. < 20 °C. EPR (benzene): 3 lines, $g = 2.007$, $a_N = 1.56$ mT. FAB-HRMS: m/z (calcd. for $C_{41}H_{65}N_2O_2$):619.5203; found 619.5220 [M + 2].

18: Yield 45%, orange powdery solid, m.p. 82−86 °C. EPR (benzene): 3 lines, $g = 2.006$, $a_N = 1.61$ mT. FAB-HRMS: m/z (calcd. for $C_{50}H_{83}N_2O_3$):761.6561; found 761.6475 [M + 2].

19: Yield 43%, orange powdery solid, m.p. 46−49 °C. EPR (benzene): 3 lines, $g = 2.007$, $a_N = 1.61$ mT. FAB-HRMS: m/z (calcd. for $C_{47}H_{77}N_2O_2$): 703.6141; found 703.6206 [M + 2].

Crystal Structure Determination of Compounds 4 and 13: Single crystals suitable for X-ray diffraction were obtained for **4** and **13** and their crystal data are as follows:

4: $C_{66}H_{96}N_4O_6$, $M = 1041.51$, triclinic, $a = 14.465(7)$ Å, $b = 23.19(1)$ Å, $c = 10.038(2)$ Å, $\alpha = 100.60(2)°$, $\beta = 94.02(4)°$, $r = 100.27(3)$, $U = 3238(2)$ Å^3, $T = 295$ K, space group $P\bar{1}$, $Z = 2$, $Dc = 1.068$ g·cm^{-3}. $R = 0.111$, $wR = 0.101$ [2595 observed reflections and 686 parameters, $I>3\sigma(I)$].

13: $C_{30}H_{43}N_2O_2$, $M = 436.68$, monoclinic, $a = 62.21(1)$ Å, $b = 11.206(6)$ Å, $c = 16.286(3)$ Å, $\beta = 94.44(2)°$, $U = 11320(6)$ Å^3, $T = 295$ K, space group $C2/c$, $Z = 16$, $Dc = 1.088$ g·cm^{-3}. $R = 0.171$, $wR = 0.145$ [3320 observed reflections and 614 parameters, $I>3\sigma(I)$].

Acknowledgments

We thank Prof. Hayao Kobayashi and his group at the Institute for Molecular Sciences for allowing us to use his X-ray facility. We are also grateful to Dr. Keiji Negita of Fukuoka University for his kind help with the estimation of LC properties. This work was supported by a Grant-in-Aid for Scientific Research on Priority Area (A) "Creation of Delocalized Electronic Systems" (No. 10146250) from the Ministry of Education, Science, Sports and Culture, Japan.

[1] [1a] O. Kahn, C. J. Martinez, *Science* **1998**, *279*, 44−48. [1b] K. Hamachi, K. Matsuda, T. Itoh, H. Iwamura, *Bull. Chem. Soc. Jpn.* **1998**, *71*, 2937−2943. [1c] W. Fujita, K. Awaga, *Science* **1999**, *286*, 261−262. [1d] K. Matsuda, M. Irie, *Chem. Lett.* **2000**, 16−17. [1e] K. Matsuda, M. Irie, *J. Am. Chem. Soc.* **2000**, *122*, 7195−7201. [1f] K. Matsuda, M. Irie, *J. Am. Chem. Soc.* **2000**, *122*, 8309−8310. [1g] T. Sugano, *Chem. Lett.* **2001**, 32−33. [1h] I. Ratera, D. Ruiz-Molina, J. Vidal-Gancedo, K.

Wurst, N. Daro, J-F. Lètard, C. Rovira, J. Veciana, *Angew. Chem. Int. Ed.* **2001**, *40*, 919−922.
[2] S. Nakatsuji, H. Anzai, *J. Mater. Chem.* **1997**, *7*, 2161−2174.
[3] [3a] S. Nakatsuji, *Adv. Mater.* **2001**, *13*, 1719−1724. [3b] S. Nakatsuji, in *Recent Research Developments in Organic & Bioorganic Chemistry* (Ed.: S. G. Pandalai), Transworld Research Network, Trivandrum, 2002, vol. 4, in press.
[4] A preliminary communication has appeared: M. Mizumoto, H. Ikemoto, H. Akutsu, J. Yamada, S. Nakatsuji, *Mol. Cryst. Liq. Cryst.* **2001**, *363*, 149−156.
[5] P. Kaszynski, in *Magnetic Properties of Organic Materials* (Ed.: P. M. Lahti), Marcel Dekker, New York, Basel, **1999**, chapter 15, p. 305−324.
[6] [6a] M. Dvolaitzky, J. Billard, F. Poldy, *C. R. Acad. Sc., Ser. C* **1974**, *279*, 533−535. [6b] M. Dvolaitzky, J. Billard, F. Poldy, *Tetrahedron* **1976**, *32*, 1835−1838.
[7] [7a] N. Tamaoki, A. Parfenov, A. Masaki, H. Matsuda, *Adv. Mater.* **1997**, *9*, 1102−1104. [7b] C. T. Imrie, G. R. Luckhurst, in *Handbook of Liquid Crystals* (Eds. D. Demus, J. Goodby, G. W. Gray, H.-W. Spiess, V. Vill), Wiley-VCH, Weinheim, **1998**, vol. 2B, p. 801−833.
[8] S. Nakatsuji, M. Mizumoto, A. Takai, H. Anzai, Y. Teki, K. Tajima, *Mol. Cryst. Liq. Cryst.* **1999**, *334*, 205−210.
[9] The high *R* factors of **4** and **13** are due partially to the poor crystallinity of the compounds and also to the fact that the alkyl chains are highly disordered, as often seen in liquid crystalline compounds with long alkyl chain; see: K. Hori, K. Endo, *Bull. Chem. Soc. Jpn.* **1993**, *66*, 46−50.
[10] [10a] J. Veciana, J. Cirujeda, C. Rovira, J. Vidal-Gancedo, *Adv. Mater.* **1995**, *7*, 221−225. [10b] K. Tagashi, R. Imachi, K. Tomioka, H. Tsuboi, T. Ishida, T. Nogami, N. Takeda, M. Ishikawa, *Bull. Chem. Soc. Jpn.* **1996**, *69*, 2821−2830. [10c] M. M. Matsushita, A. Izuoka, T. Sugawara, T. Kobayashi, T. Wada, N. Takeda, M. Ishikawa, *J. Am. Chem. Soc.* **1997**, *119*, 4369−4379.
[11] R. H. Pearson, I. Pascher, *Nature* **1979**, *281*, 499−501.
[12] A similar magnetic behavior was observed in an EPR measurement in the heating process around the mesogenic phase i.e. an apparent increase of the line width was observed around the phase.
[13] An opposite change of magnetic behavior (from Curie−Weiss to ST) has been found in another radical compound: H. Ikemoto, H. Akutsu, J. Yamada, S. Nakatsuji, *Tetrahedron Lett.* **2001**, *42*, 6873−6875.
[14] S. Nakatsuji, A. Takai, K. Nishikawa, Y. Morimoto, N. Yasuoka, K. Suzuki, T. Enoki, H. Anzai, *J. Mater. Chem.* **1999**, *9*, 1747−1754.
[15] Software package: teXsan Crystal Structure Analysis Package, Windows version 1.06, Molecular Structure Corporation, **1997**−**1999**.
[16] S. Nakatsuji, T. Ojima, H. Akutsu, J. Yamada, *J. Org. Chem.* **2002**, *67*, 916−921.
[17] Since some of the solid samples in this class of radical compounds turned to tarry materials during the recrystallization, due probably to gradual decomposition, no elemental analysis data are available for the samples.
[18] The appearance of the [M + 2] peak as the main peak has been observed in the FAB-MS measurements for this class of radical compounds in general, and we then adjusted the FAB-HRMS data generally to the main peak.

Received January 25, 2002
[O02037]